

A Theory of the High-Mode Phenomenon for Stellarators*

K. C. Shaing

Oak Ridge National Laboratory, Oak Ridge, Tennessee 37831-8071

ABSTRACT

It is shown that besides the ion orbit loss mechanism, which occurs in a region $a - \varepsilon_i \rho_p < r < a$, the collisionless drift-orbit transport flux can also drive the poloidal $\vec{E} \times \vec{B}$ velocity in a region $r < a - \varepsilon_i \rho_p$ in stellarators. Here, r is the minor radius, a is the plasma radius, ε_i is the toroidal amplitude of the magnetic field spectrum, \vec{E} is the electric field, \vec{B} is the magnetic field, and ρ_p is the poloidal ion gyroradius. The transport-flux-driven $\vec{E} \times \vec{B}$ velocity can be triggered most efficiently by an increase of the ion temperature gradient. The theory is applied to the high-mode (H-mode) phenomenon observed in stellarators.

The high-mode (H-mode) phenomenon has been observed in both tokamaks and stellarators.¹⁻⁶ The general behavior is similar in both kinds of devices. It can be understood by a logical sequence originally proposed in Refs. 7 and 8. First, the poloidal $\vec{E} \times \vec{B}$ flow velocity driven by the ion orbit loss bifurcates over the local maximum of the plasma viscosity located at $M_p \approx 1$. Here, \vec{E} is the electric field, \vec{B} is the magnetic field, and M_p is the poloidal $\vec{E} \times \vec{B}$ Mach number. Second, the turbulence fluctuation is suppressed by the radial gradients of the $\vec{E} \times \vec{B}$ angular velocity and the diamagnetic angular velocity, and the plasma confinement is thus improved. The results of this simple theory are in agreement with many H-mode phenomena observed in tokamaks. However, the theory may not adequately explain some of experimental results because realistic plasmas usually have neutral particles, magnetic islands, error fields, and other "non-ideal" effects in the edge region. Incorporating these realistic plasma conditions in the theory produces better agreement between the theory and the experimental results, as demonstrated in Refs. 9 and 10. The absence of unquantifiable parameters from the transition theory is what makes possible the comparisons with experimental results.

This letter is directed toward pursuing this quantitative theory to explore the consequences of the differences between tokamak and stellarator transport properties. It is shown that in stellarators the poloidal $\vec{E} \times \vec{B}$ velocity can be driven to bifurcation not only by the ion orbit loss mechanism but also by the collisionless drift-orbit transport flux. The collisionless drift-orbit transport flux is the radial particle flux driven by the collisionless helically trapped particles. The ion orbit loss mechanism is important only in the region where $a - \varepsilon_i \rho_p < r < a$, where a is the plasma minor radius, r is the local minor radius, ε_i is the toroidal amplitude of the model magnetic field spectrum $B = B_0 [1 - \varepsilon_i \cos \theta - \varepsilon_h \cos(m\theta - n\zeta)]$, B_0 is the magnetic field strength on the axis, ε_h is the helical amplitude, (m, n) is the poloidal and toroidal mode numbers of the helical magnetic field, and ρ_p is the ion poloidal gyroradius. In this region, the bifurcation of the $\vec{E} \times \vec{B}$ velocity in stellarators is similar to that in tokamaks and is not discussed in detail.

* Research sponsored by the Office of Fusion Energy, U.S. Department of Energy, under contract DE-AC05-84OR21400 with Lockheed Martin Energy Systems, Inc.

DISCLAIMER

This report was prepared as an account of work sponsored by an agency of the United States Government. Neither the United States Government nor any agency thereof, nor any of their employees, make any warranty, express or implied, or assumes any legal liability or responsibility for the accuracy, completeness, or usefulness of any information, apparatus, product, or process disclosed, or represents that its use would not infringe privately owned rights. Reference herein to any specific commercial product, process, or service by trade name, trademark, manufacturer, or otherwise does not necessarily constitute or imply its endorsement, recommendation, or favoring by the United States Government or any agency thereof. The views and opinions of authors expressed herein do not necessarily state or reflect those of the United States Government or any agency thereof.

DISCLAIMER

Portions of this document may be illegible in electronic image products. Images are produced from the best available original document.

However, in the region $r < a - \varepsilon_i \rho_p$, the collisionless ion drift-orbit transport flux can also drive the poloidal $\vec{E} \times \vec{B}$ velocity to bifurcation. This bifurcation mechanism does not exist in axisymmetric tokamaks. It can be triggered most efficiently by an increase in the ion temperature gradient. A similar mechanism was employed in Ref. 11 to show that the sign of the radial electric field E_r can be positive¹² in H-mode in a rippled tokamak owing to the electron drift-orbit transport flux.

The poloidal and toroidal components of the momentum equation in Hamada coordinates¹³ in a toroidal plasma are

$$NM \partial \langle \vec{B}_p \cdot \vec{V} \rangle / \partial t = - \langle \vec{B}_p \cdot \nabla \cdot \pi \rangle - v_{\text{eff}} NM \langle \vec{B}_p \cdot \vec{V} \rangle - \frac{\psi' x'}{c} \langle \vec{J} \cdot \nabla V \rangle, \quad (1)$$

$$NM \partial \langle \vec{B}_t \cdot \vec{V} \rangle / \partial t = - \langle \vec{B}_t \cdot \nabla \cdot \pi \rangle - v_{\text{eff}} NM \langle \vec{B}_t \cdot \vec{V} \rangle + \frac{\psi' x'}{c} \langle \vec{J} \cdot \nabla V \rangle, \quad (2)$$

where the angular brackets denote the flux surface average, N is the plasma density, M is the ion mass, π is the viscous tensor, \vec{J} is the current density, c is the speed of light, $\vec{B}_t = \psi' \nabla V \times \nabla \theta$, $\vec{B}_p = -x' \nabla V \times \nabla \zeta$, $\psi' = \vec{B} \cdot \nabla \zeta$, $x' = \vec{B} \cdot \nabla \theta$, V is the volume enclosed in the flux surface, and θ and ζ are poloidal and toroidal angle, respectively. The radial current density $\langle \vec{J} \cdot \nabla V \rangle$ in Eqs. (1) and (2) is related to $\partial \langle \vec{E} \cdot \nabla V \rangle / \partial t$ through Ampère's law $\langle \vec{J} \cdot \nabla V \rangle = -(1/4\pi) \partial \langle \vec{E} \cdot \nabla V \rangle / \partial t$. The effective collision frequency of the charge-exchange momentum loss is defined as $v_{\text{eff}} = N_n \langle \sigma v \rangle_{\text{cx}}$, where N_n is the neutral density and $\langle \sigma v \rangle_{\text{cx}}$ is the charge-exchange reaction cross section.¹⁴

The plasma viscous forces $\langle \vec{B}_p \cdot \nabla \cdot \pi \rangle$ and $\langle \vec{B}_t \cdot \nabla \cdot \pi \rangle$ contains information about the ion orbit loss, the collisionless drift-orbit transport flux, and the nonlinear collisional viscosities. The nonlinear collisional viscosities are from particles in the plateau-fluid-Pfirsch-Schlüter regime.¹⁵ The particles in the collisionless regime contribute to either the ion orbit loss or the drift-orbit transport flux, depending on how far they are from the plasma boundary. The relevant collisionality parameter here is v_*^h for the helically trapped particles, defined as $v_*^h = \nu R q / (\varepsilon_h^{3/2} v_i |m - nq|)$, where ν is the ion-ion collision frequency, R is the major radius, q is the safety factor, v_i is the ion thermal speed, and m and n are the poloidal and toroidal mode numbers of the helical amplitude of the magnetic field spectrum. When $v_*^h < 1$, the helically trapped particles become collisionless. We assume that $nq \gg m$, which leads us to conclude that the conventional ion collisionality of the toroidally trapped particles v_* is larger than v_*^h if $\varepsilon_t \approx \varepsilon_h$, where ε_t and ε_h are the amplitudes of the toroidal and helical components of the magnetic field spectrum. This indicates that the most relevant particle orbit topology for the stellarator H-mode is that of the helically trapped particles. The radial drift-orbit size Δr of the helically trapped particles in the presence of the poloidal $\vec{E} \times \vec{B}$ drift is of the order of

$$\Delta r \approx v_{dr} \Delta t, \quad (3)$$

where v_{dr} is the bounce-averaged radial drift velocity and Δt is the period of the drift orbit. Because the poloidal $\vec{E} \times \vec{B}$ velocity is larger than the $\nabla \vec{B}$ and curvature drifts if $e\Phi/T \approx 1$, Δt is of the order of r/V_E with $V_E = cE_r/B$. Here, Φ is the electrostatic potential, $B = |\vec{B}|$, e is the charge of the ions, and T is the ion temperature. Note that $v_{dr} \approx v^2/(2\Omega R)$ with v the particle speed, and Ω the ion gyrofrequency, one concludes that

$$\Delta r \approx \varepsilon_i \rho_p / M_p, \quad (4)$$

where M_p is the poloidal $\vec{E} \times \vec{B}$ Mach number defined as $V_E B / v_i B_p$. Because at the H-mode bifurcation M_p is of the order of unity, the helically trapped drift ion orbits can intersect the plasma boundary if they are within a distance $\varepsilon_i \rho_p$ away from the boundary;

that is, if they are in the region $a - \varepsilon_i \rho_p < r < a$. If they are in the region $r < a - \varepsilon_i \rho_p$, they cannot intersect the plasma boundary when $M_p \approx 1$. In that case the physical consequence of their contribution to plasma viscosities is the well-known collisionless transport flux discussed extensively in Refs. 16 and 17. The relationship between the drift-orbit transport flux and the plasma viscosities is shown to be¹⁸

$$\langle \vec{\Gamma} \cdot \nabla V \rangle_{non} = -\frac{c}{ex' \psi'} \langle \vec{B}_p \cdot \nabla \cdot \pi \rangle = \frac{c}{ex' \psi'} \langle \vec{B}_t \cdot \nabla \cdot \pi \rangle, \quad (5)$$

where $\langle \vec{\Gamma} \cdot \nabla V \rangle_{non}$ is the radial component of the drift-orbit transport flux. In general, $\langle \vec{\Gamma} \cdot \nabla V \rangle_{non}$ consists of three regimes as shown in Ref. 16. Here, for simplicity, we employ only the $1/\nu$ regime flux to demonstrate the bifurcation of the poloidal $\vec{E} \times \vec{B}$ velocity for H-mode application.

In the cylindrical coordinates (r, θ, ζ) , Eq. (5) can be expressed as

$$\langle \vec{B}_p \cdot \nabla \cdot \pi \rangle = -\langle \vec{B}_t \cdot \nabla \cdot \pi \rangle = -\frac{e}{c} B_p B \Gamma_r, \quad (6)$$

where $B_p = |\vec{B}_p|$ and Γ_r is the radial component of the particle flux. The particle flux in the $1/\nu$ regime is¹⁷

$$\Gamma_r = -\frac{64}{9(2\pi)^{3/2}} N \varepsilon_h^{3/2} \varepsilon_t^2 \left(\frac{cT}{eBr} \right)^2 \frac{1}{\nu} \left[I_{-1} \left(\frac{P'}{P} + \frac{e\Phi'}{T} \right) + I_{-2} \frac{T'}{T} \right], \quad (7)$$

where $P = NT$ is the ion pressure, $P' = dP/dr$, $T' = dT/dr$, $\Phi' = d\Phi/dr$, and the integrals I_{-1} and I_{-2} are defined as

$$\begin{cases} I_{-1} \\ I_{-2} \end{cases} = \int_{\sqrt{y^h}}^{\infty} dy y^4 \begin{cases} 1 \\ y - \frac{5}{2} \end{cases} e^{-y}.$$

At the steady state, Eqs. (1) and (2) in cylindrical coordinates become

$$\begin{aligned} & -\frac{32}{9(2\pi)^{3/2}} \frac{\varepsilon_t^2}{|m-nq| v_*^h} \left[I_{-1} (M_p - V_{p,p}) - I_{-2} V_{p,T} \right] \\ & = \frac{\sqrt{\pi}}{4} \sum_{mn} \varepsilon_{mn}^2 m(m-nq) \left\{ I_{mn} \left[\frac{V_{\parallel}}{v_i} + \frac{m}{m-nq} (M_p - V_{p,p}) \right] - L_{mn} \frac{m}{m-nq} V_{p,T} \right\} \\ & \quad + \varepsilon_t^2 \frac{v_{eff}}{v_i / Rq} \left[\frac{V_{\parallel}}{v_i} + \frac{1+2q^2}{q^2} (M_p - V_{p,p}) \right], \end{aligned} \quad (8)$$

$$\begin{aligned} & \frac{32}{9(2\pi)^{3/2}} \frac{\varepsilon_t^2}{|m-nq| v_*^h} \left[I_{-1} (M_p - V_{p,p}) - I_{-2} V_{p,T} \right] \\ & = \frac{\sqrt{\pi}}{4} \sum_{mn} \varepsilon_{mn}^2 nq(nq-m) \left\{ I_{mn} \left[\frac{V_{\parallel}}{v_i} + \frac{m}{m-nq} (M_p - V_{p,p}) \right] - L_{mn} \frac{m}{m-nq} V_{p,T} \right\} \\ & \quad + \frac{v_{eff}}{v_i / Rq} \frac{V_{\parallel}}{v_i}, \end{aligned} \quad (9)$$

where V_{\parallel} is the parallel (to \vec{B}) flow speed, $M_p = -cE_r/B_p v_i$, $V_{p,p} = -cP'/Ne v_i B_p$, $V_{p,T} = -cT'/e v_i B_p$, and ε_{mn} is the Fourier amplitude of the magnetic field spectrum $B = B_0 [1 + \sum_{mn} \varepsilon_{mn} \cos(m\theta - n\zeta)]$. The integrals I_{mn} and L_{mn} in Eqs. (8) and (9) are defined as

$$\begin{Bmatrix} I_{mn} \\ L_{mn} \end{Bmatrix} = \frac{1}{\pi} \int_0^{\sqrt{v_k^2}} dx x^2 e^{-x} \begin{Bmatrix} 1 \\ x - \frac{5}{2} \end{Bmatrix} \int_{-1}^1 dy (1-3y^2)^2 \left(\frac{vx'}{B} \right) R_{mn}$$

where $R_{mn} = v_k / \left[(m\omega_\theta - n\omega_\zeta)^2 + v_k^2 \right]$, $\omega_\theta = (v_\parallel + V_\parallel)x'/B + \bar{V}_E \cdot \nabla\theta$, $\omega_\zeta = (v_\parallel + V_\parallel)\psi'/B + \bar{V}_E \cdot \nabla\zeta$, v_\parallel is the parallel particle speed, $v_k = 3v_D + v_E + v_{eff}$, v_D is the deflection frequency,¹⁹ and v_E is the energy exchange frequency.¹⁹ Note that we have employed the poloidal and toroidal viscosities calculated in Hamada coordinates in Ref. 15 from the solution of the drift kinetic equation and the definitions given in Ref. 20 and converted the results to the cylindrical coordinates based on the conversion formula derived for a large-aspect-ratio tokamak in Ref. 21. Note that the energy integrals I_{mn} and L_{mn} are truncated. This indicates that we are assuming that the particle distribution function is a Maxwellian. The hot particles contribute to drift-orbit transport flux, and the cold particles contribute to the collisional viscosities. For simplicity, we use the simple model field $B = B_0 [1 - \varepsilon_t \cos\theta - \varepsilon_h \cos(m\theta - n\zeta)]$. We also assume that the toroidal flow speed $V_t \approx V_\parallel$ is heavily damped by toroidal viscous force and charge-exchange momentum loss so that $V_t/v_t \approx V_\parallel/v_t \approx 0$. However, this assumption is not necessary. The bifurcation solutions for the coupled nonlinear Equations (8) and (9) will be presented separately. With this simplification Eq. (8) becomes a nonlinear equation of M_p for the set of plasma parameters employed. This equation is solved by plotting the left and the right sides of Eq. (8) as functions of M_p . The solution is the intersection of these two curves. For the plasmas parameters, similar to those of Wendelstein 7-AS, $\varepsilon_t = 0.053$, $\varepsilon_h = 0.025$, $q = 1.92$, $m = 2$, $n = 5$, and $v_{eff} = 0.01$, the results are shown in Figs. 1–3.

In Fig. 1, the collisionality is high, $\nu_* = 15$, and $V_{p,p} = V_{p,T} = 0.25$. The $\bar{E} \times \bar{B}$ Mach number is subsonic for these parameters. This is the Low-mode (L-mode) solution. When the collisionality decreases from the Pfirsch-Schlüter regime to the plateau regime, the neoclassical ion energy confinement improves which leads to higher values of ion temperature and ion temperature gradient dT/dr . In that case, the value of M_p increases. If the ion collisionality keeps decreasing, there can be three equilibrium solutions for M_p , as shown in Fig. 2, where $V_{p,p} = V_{p,T} = 0.50$ and $\nu_* = 7.5$. The one with the smallest value is the continuation of the L-mode solution. The one with the largest value is the new H-mode solution. Both of these solutions are stable. The one in the middle is unstable and is not relevant. If the ion collisionality decreases further to $\nu_* = 7.0$, only the H-mode solution exists, as shown in Fig. 3, where $V_{p,p} = V_{p,T} = 0.55$. Note that the H-mode solution has $M_p \approx 2$.

One can easily conclude that increasing the ion temperature gradient is more efficient than increasing the density gradient in driving M_p to the H-mode value. The reason is that the magnitude of I_{-2} is about a factor of 2.5 larger than I_{-1} . Thus, the increase in dT/dr needed to push the zero of the left side of Eq. (8) to a higher value, to facilitate bifurcation, is smaller than the necessary increase in dN/dr . Furthermore, the ion energy confinement in the edge region could be close to be neoclassical. In that case, lower ion collisionality can improve the ion energy confinement and increase dT/dr . However, particle confinement in the edge region is likely to be anomalous. Lower ion collisionality may not increase dN/dr . After H-mode bifurcation, particle confinement should improve, and dN/dr should increase.

We emphasize that the process described here is applicable in the region $r < a - \varepsilon_t \rho_p$. Because $\varepsilon_t \rho_p$ is much less than 1 cm for typical edge parameters, this is the region that is most likely to be measured with limited spatial resolution. Only in the region

$a - \varepsilon_i \rho_p < r < a$ can the ion orbit loss process be observed. As noted earlier, the drift-orbit-transport-driven $\vec{E} \times \vec{B}$ flow only exists in non-axisymmetric toroidal plasmas such as stellarators and not in axisymmetric tokamaks.

We summarize the H-mode transition sequence in the region $r < a - \varepsilon_i \rho_p$ in stellarators as follows:

1. The ion collisionality decreases due to plasma heating, which leads to higher values of T and dT/dr .
2. Lower collisionality and larger dT/dr drive the poloidal $\vec{E} \times \vec{B}$ flow to bifurcation.
3. Plasma confinement is improved because of the gradients of the poloidal $\vec{E} \times \vec{B}$ angular velocity and the diamagnetic angular velocity which suppress turbulence.

REFERENCES

- ¹ASDEX Team, Nucl. Fusion **29**, 1959 (1989).
- ²R. J. Taylor, M. L. Brown, B. D. Fried, H. Grote, J. R. Liberati, G. J. Morales, P. Pribyl, D. Darrow, and M. Ono, Phys. Rev. Lett. **63**, 2365 (1989).
- ³R. J. Groebner, K. H. Burrell, and R. P. Seraydarian, Phys. Rev. Lett. **64**, 3015 (1990).
- ⁴K. Ida, S. Hidekuma, Y. Miura, T. Fujita, M. Mori, K. Hoshino, N. Suzuki, T. Yamauchi, and JFT-2M Group, Phys. Rev. Lett. **65**, 1364 (1990).
- ⁵F. Wagner, J. Baldzuhn, R. Brakel, R. Burhenn, V. Erckmann, T. Estrada, P. Grigull, H. J. Hartfuss, G. Herre, M. Hirsch, J. V. Hofmann, R. Jaenicke, A. Rudyj, U. Stroth, A. Weller, and the W7-AS Teams, Plasma Phys. Controlled Fusion **36**, A61 (1994).
- ⁶K. Toi, T. Morisaki, S. Sakakibara, A. Ejiri, H. Yamada, S. Morita, K. Tanaka, N. Nakajima, S. Okamura, H. Iguchi, K. Ida, K. Tsumori, S. Ohdachi, K. Nishimura, K. Matsuoka, J. Xu, I. Yamada, T. Minami, K. Narihara, R. Akiyama, A. Ando, H. Arimoto, A. Fujisawa, M. Fujiwara, H. Idei, O. Kaneko, K. Kawahata, A. Komori, S. Kubo, R. Kumazawa, T. Ozaki, S. Sagara, C. Takahashi, Y. Takita, and T. Watari, in *Proceedings of the 15th International Conference on Plasma Physics and Controlled Nuclear Fusion Research*, Seville, 1994 (International Atomic Energy Agency, Vienna, in press).
- ⁷K. C. Shaing and E. C. Crume, Jr., Phys. Rev. Lett. **63**, 2369 (1989).
- ⁸K. C. Shaing, E. C. Crume, Jr., and W. A. Houlberg, Phys. Fluids B **2**, 1496 (1990).
- ⁹K. C. Shaing and C. T. Hsu, "Critical Neutral Density for High-Mode Bifurcation in Tokamaks," (to be published in Phys. Plasmas, 1995).
- ¹⁰K. C. Shaing and Y. Z. Zhang, "Transition to High-Mode Induced by Reduction of Magnetic Stress," (to be published in Phys. Plasmas, 1995).
- ¹¹K. Itoh and S.-I. Itoh, Nucl. Fusion **32**, 2243 (1992).
- ¹²S.-I. Itoh and K. Itoh, Phys. Rev. Lett. **60**, 2376 (1988).
- ¹³S. Hamada, Prog. Theoret. Phys. (Kyoto) **22**, 145 (1959).
- ¹⁴M. Coronado and J. N. Talmadge, Phys. Fluids B **5**, 1200 (1993).
- ¹⁵K. C. Shaing, Phys. Fluids B **5**, 3841 (1993).
- ¹⁶A. A. Galeev and R. Z. Sagdeev, in *Advances in Plasma Physics* (A. Simon and W. B. Thompson, eds., John Wiley & Sons, New York, 1976), Vol. 6, p. 311.
- ¹⁷J. W. Connor and R. J. Hastie, Nucl. Fusion **13**, 221 (1973).
- ¹⁸K. C. Shaing and J. D. Callen, Phys. Fluids **26**, 3315 (1983).
- ¹⁹S. P. Hirshman and D. J. Sigmar, Nucl. Fusion **21**, 1079 (1976).
- ²⁰M. Coronado and H. Wobig, Phys. Fluids **29**, 527 (1986).
- ²¹M. Coronado and J. Galindo Trejo, Phys. Fluids B **2**, 530 (1990).

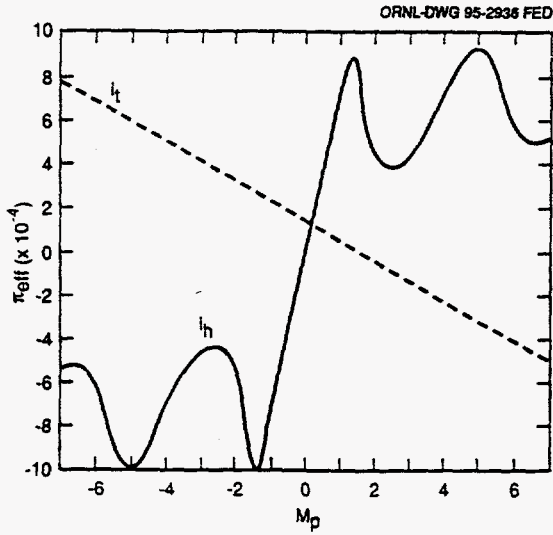


Fig. 1. The left side (I_l) and the right side (I_r) of Eq. (8) versus M_p for $\nu_s = 15$, $\epsilon_1 = 0.053$, $\epsilon_2 = 0.025$, $q = 1.92$, $m = 2$, $n = 5$, $V_{p,q} = 0.01$, and $V_{p,p} = V_{p,r} = 0.25$. There is only one equilibrium solution of M_p for these parameters.

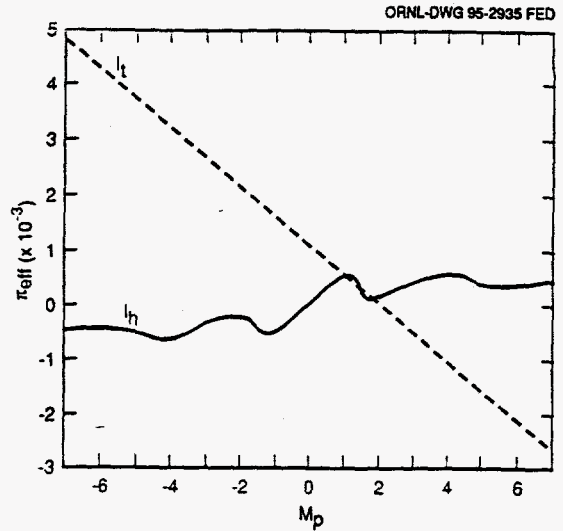


Fig. 2. I_l and I_r versus M_p for the same parameters as in Fig. 1 except $\nu_s = 7.5$ and $V_{p,p} = V_{p,r} = 0.50$. There are three equilibrium solutions of M_p . The one in the middle is unstable.

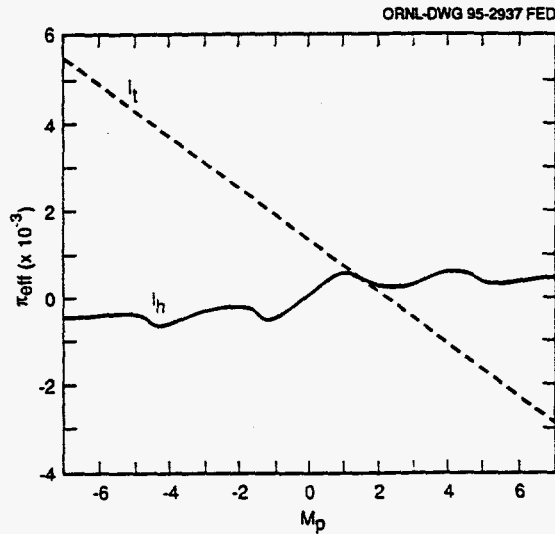


Fig. 3. I_l and I_r versus M_p for the same parameters as in Fig. 1 except $\nu_s = 7.0$ and $V_{p,p} = V_{p,r} = 0.55$. There is only one equilibrium solution of M_p .

DISCLAIMER

This report was prepared as an account of work sponsored by an agency of the United States Government. Neither the United States Government nor any agency thereof, nor any of their employees, makes any warranty, express or implied, or assumes any legal liability or responsibility for the accuracy, completeness, or usefulness of any information, apparatus, product, or process disclosed, or represents that its use would not infringe privately owned rights. Reference herein to any specific commercial product, process, or service by trade name, trademark, manufacturer, or otherwise does not necessarily constitute or imply its endorsement, recommendation, or favoring by the United States Government or any agency thereof. The views and opinions of authors expressed herein do not necessarily state or reflect those of the United States Government or any agency thereof.